Asian Journal of Chemistry Vol. 22, No. 2 (2010), 893-901

Synthesis, Characterization and Electrochemical Study of Transition Metals [Cu(II), Fe(III)] Complexes of Fumarate 2,9-Dimethyl-1,10-phenanthroline

QINGZHU CHU, MEILING ZHANG and CAIFENG DING*
College of Chemistry and Molecular Engineering,
Qingdao University of Science and Technology, Qingdao-266042, Shandong, P.R. China
Tel/Fax: (86)(532)84022750; E-mail: dingcaifeng2003@163.com; baochai76@yahoo.com.cn

Two new complexes containing 2,9-dimethyl-1,10-phenanthroline (phen), fumarate and transition metals, $Cu_2(phen)_2(fumarate)(H_2O)_2]Cl_2$ (**1**), $[Fe_2(phen)_2(fumarate)(H_2O)_2](NO_3)_4$ (**2**), were synthesized and characterized. The crystal structure of compound **1** was determined by X-ray crystallography. The thermal decomposition was studied by thermal analysis TG-DTG. The interaction of these complexes with DNA was studied by cyclic voltammetry (CV) and differential pulse voltammetry (DPV). The electrochemical experimental results indicate that these complexes could interact with DNA.

Key Words: Complexes, Crystal structure, Thermal analysis, Electrochemical study, DNA.

INTRODUCTION

1,10-Phenanthroline is a well-known N-heterocyclic chelating agent with a rigid planar structure. Currently, in the field of supramolecular chemistry, 1,10-phenanthroline units, as an important building block, play an important role for the development of the supramolecular chemistry[1-3]. Many novel supramolecular compounds contaning 1,10-phenanthroline units. At the same time several metal complexes with 1,10-phenanthroline and natural products incorporating this heterocyclic nucleus possess interesting anticancer properties[4-7].

Binding studies of transition metal complexes have become a very important field in the development of DNA molecule probes and chemotherapeutics[8-13]. Among these complexes, metals or ligands can be varied in an easily controlled way to facilitate the individual applications[14-17]. Basically, metal complexes interact with double helix DNA in either noncovalent or covalent way. The former way includes three binding modes, *i.e.*, intercalation, groove binding and external statiction electronic effects. Among these interactions, intercalation is one of the most important DNA binding modes. It was reported that the intercalating ability appeared to increase with the improvement in planarity of ligands[18,19]. Additionally, the coordination geometry and ligand donor atom also play key roles in determining the binding

extent of complexes to DNA[20,21]. The metal ion and its flexible valence, which are responsible for the geometry of complexes, also affect the intercalating ability of metal complexes to DNA[22,23].

Transition metal complexes using 1,10-phenanthroline as ligands are capable of selectively binding DNA through interaction[24-26]. 2,9-Dimethyl-1,10-phenanthroline transition metal complexes have the ability of distinguishing and splitting DNA and could be used as chemical nucleases[27-30]. Recently we have obtained four new 2,9-dimethyl-1,10-phenanthroline transition metal complexes. Herein, we reported their crystal structures, thermal stability and electrochemical behaviour.

EXPERIMENTAL

Transition metal salt $CuCl_2 \cdot 2H_2O$ and $Fe(NO_3)_3 \cdot 9H_2O$ were used in this experiment, respectively. Double-stranded salmon sperm DNA was purchased from Shanghai Huashun Biological Engineering Company ($A_{260}/A_{280} > 1.8$). Other reagents used in this work were AR grade and were used without further purification. Elemental analyses were performed on a Vario EL III elemental analyzer. The ^1H NMR spectrum was recorded on Bruker AV500 NMR spectrometer and DMSO-d_6 was used as the solvent, tetramethylsilane (TMS) was used as an internal standard. The thermogravimetric analysis (TGA) was performed with a thermal analyzer of NETZSCH TG209. Electrochemical studies were performed on CHI 832B electrochemical analyzer.

Synthesis of complexes: 5 mL of aqueous solution of transition metal salt (2 mmol) was added dropwise to 30 mL of ethanol solution of 2,9-dimethyl-1,10-phenanthroline (0.416 g, 2 mmol) and fumaric acid (0.116 g, 1 mmol) with constant stirring. The mixture was filtered after being heated and refluxed for 1 h. The filtrate was left to stand undisturbed and slow evaporation at room temperature for two weeks. Crystal suitable for X-ray diffraction analysis were obtained.

Complex 1: Anal. calcd. (%) for $Cu_2(C_{14}H_{12}N_2)_2(C_4H_2O_4^{2-})Cl_2 \cdot 4H_2O$: C 48.00, H 4.28, N 7.00; found C 49.79, H 4.33, N 6.86.

Complex 2: Anal. calcd. (%) for $Fe_2(C_{14}H_{12}N_2)_2(C_4H_2O_4^{2-})(NO_3^-)_4 \cdot 2H_2O$: C 41.49, H 3.20, N 12.10; found C 41.33, H 3.41, N 11.93. ^1H NMR (DMSO, 500 Hz): 1.10 (s, 4H), 3.066 (s, 12H), 6.51 (b, 2H), 8.082-8.098 (b, 4H), 8.256 (s, 4H), 8.912-8.928 (b, 4H).

Crystallographic study: The single crystal of **1** was mounted on a SMART 1000 CCD diffractometer. Reflection data was measured at 293(2) K using MoK_α radiation ($\lambda = 0.071073$ nm) with a graphite monochromator. The technique used was ω-scan with limits $1.87 < \theta < 26.0$ for complex one. Empirical absorption correction was carried out by the SADABS program[9]. The structure was solved by direct methods and refined by least squares on F^2 using the SHELXTL software package. All non-hydrogen atoms were refined anisotropically and hydrogen atoms were located and included at their calculated position. Crystal parameters and refinement results are summarized in Table-1.

TABLE-1
CRYSTAL DATA AND STRUCTURE REFINEMENT PARAMETERS FOR $[C_{32}H_{30}C_{12}Cu_2N_4O_6{\cdot}2H_2O]$ AND $C_{36}H_{36}Mn_2N_4O_{10}$

Formula	$C_{32}H_{30}C_{12}Cu_2N_4O_6{\cdot}2H_2O$	D (calcd.) ($g.cm^{-3}$)	1.664
Formula weight	800.63	μ (mm^{-1})	1.557
Colour/shape	White/plate	F(000)	410
Crystal system	Triclinic	Crystal size (mm)	0.54×0.15×0.08
Space group	P-1	Temperature (K)	293
A (Å)	7.2159(8)	θ ranges (º)	1.8-26.0
b (Å)	10.4935(12)	h/k/l	-8/5; -12/12; -13/11
c (Å)	11.3180(13)	Reflections collected	4472
α (º)	83.867(2)	Independent reflections	3049
β (º)	77.765(2)	Absorption correction	Semi-empirical
γ (º)	72.773(2)	Observed data [I > 2σ(I)]	2803
V ($Å^3$)	799.07(16)	Final R indices [I > 2σ(I)]	R_1=0.0366, wR_2 =0.1199
Z	1		

Electrochemical studies between complex 1 and DNA: 0.5 mL of 1.0×10^{-4} mol/L complex **1** was added to 5 mL of 0.2 mol/L Na_2HPO_4-NaH_2PO_4 buffer solution (pH 4.5). The CV and DPV curves of complex **1** were recorded on a CHI 832B electrochemical analyzer with the three-electrode system, glassy carbon electrodes (GCE) were used as working electrode, Pt wire served as auxiliary electrode and Ag/AgCl/KCl(sat) as reference electrode. Then 20 μL 1.73×10^{-3} mol/L DNA were added to 2 mL of the above solution followed by recording the grap. Cyclic voltammetric instrument parameters were: the potential scanning range from 0.8 to 0 V. The scanning rate 0.1 V/s, the sample interval 0.001V and the quiet time 2 s. Differential pulse voltammetry instrument parameters were: the potential scanning range from 0.7 to 0.1 V, the increasing potential 0.004 V, the pulse width 0.05 s, the pulse period 0.2 s and the quiet time 2 s.

Electrochemical studies between complex 2 and DNA: 1 mL of 1.0×10^{-3} mol/L complex **2** was added to 10 mL of 0.2 mol/L HOAc-NaOAc buffer solution (pH 5.0). The CV and DPV of complex **2** were recorded on the same electrochemical analyzer. Then 20 μL 1.73×10^{-3} mol/L DNA were added to 2 mL of the above solution followed by recording the figure. CV instrument parameters were: the potential scanning range from 0.4 to -0.4 V. The scanning rate 0.1 V/s, the sample interval 0.001 V and the quiet time 2 s. DPV instrument parameters were: the potential scanning range from 0.25 to -0.27 V, the increasing potential 0.004 V, the pulse width 0.05 s, the pulse period 0.2 s and the quiet time 2 s.

RESULTS AND DISCUSSION

X-ray crystal structure of complex 1: The selected bond lengths and angles of complex **1** are list in Table-2, while the molecular structure and unit-cell paking diagram are shown in Fig. 1.

TABLE-2
SELECTED BOND LENGTHS (Å) FOR $[C_{32}H_{30}Cl_2Cu_2N_4O_6{\cdot}2H_2O]$

Bond (º)	Distance (Å)	Bond (º)	Distance (Å)
Cu(1)-C(l2)	2.2899(9)	O(2)-C(15)	1.247(3)
Cu(1)-O(1)	1.9850(2)	O(2W)-H(1WB)	0.860(5)
Cu(1)-O(2W)	1.9710(2)	O(2W)-H(2WA)	0.820(4)
Cu(1)-N(1)	2.0160(2)	O(1W)-H(1WA)	0.870(6)
Cu(1)-N(2)	2.2530(2)	O(1W)-H(2WB)	0.800(5)
O(1)-C(15)	1.2680(3)	C(10)-C(14)	1.501(5)

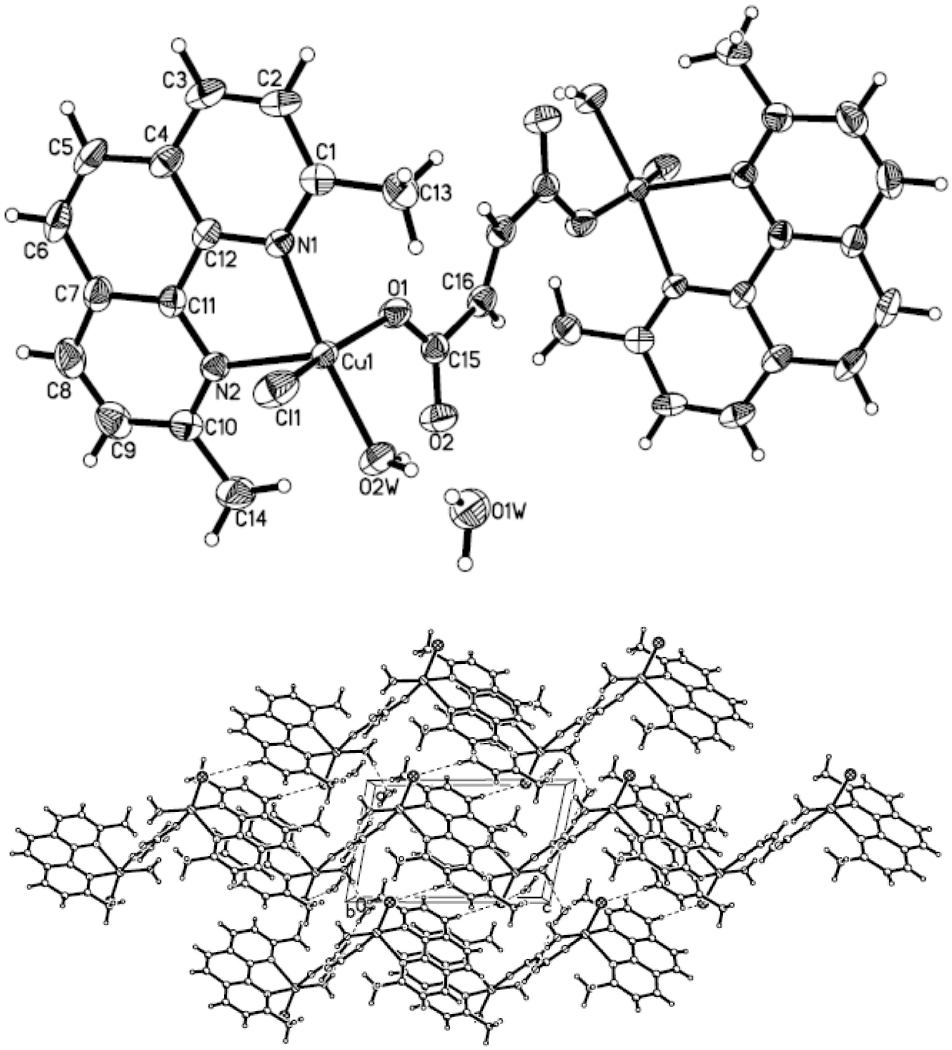

Fig. 1. Molecular structure and packing diagram of the unit cell of $[C_{32}H_{30}Cl_2Cu_2N_4O_6(H_2O)_2]$ with the atomic numbering scheme

The X-ray crystal structural studies indicated that complex **1** contains 2,9-dimethyl-1,10-phenanthroline, fumarate and water as ligands. It is a binuclear copper complex. Cu(1) and Cu(2) have completely symmetrical position. Each of them is five-coordinated by two nitrogen atoms (N(1), N(2)) of phenanthroline rings, two oxygen atoms (O(1)) of fumarate and (O(2w)) of water molecular and one chlorine atom (Cl(1)). Cu(1) and Cu(2) are linked by fumarate group in bidentate bridging fashion. The length of Cu(1)-N(1) and Cu(1)-N(2) is 2.016(2) and 2.235(2) Å and the length of Cu(1)-O(1), Cu(1)-O(2w) and Cu(1)-Cl(1) is 1.985(2), 1.971(2) and 2.2899(9) Å. There are six hydrogen-bond linkages among coordination water O(1w), O(2w) and Cl^- anions. These intermolecular hydrogen-bond distances are listed in Table-3.

TABLE-3
HYDROGEN-BONDING GEOMETRY (Å) FOR $[C_{32}H_{30}Cl_2Cu_2N_4O_6(H_2O)_2]$

D–H···A	D–H	H···A	D···A	D–H···A
O2W–H2WA···O2	0.8204	1.8776	2.637(3)	153.49
O2W–H1WB···O1W	0.86(5)	1.93(5)	2.778(4)	168(4)
O1W–H1WA···Cl2	0.87(6)	2.52(6)	3.382(3)	169(5)
O1W–H2WB···O2	0.80(5)	2.19(5)	2.968(4)	165(4)
C3–H3A···Cl2	0.9185	2.7385	3.644(3)	168.72
C14–H14A···O2W	0.9599	2.3700	3.287(4)	159.59

Symmetry codes: (i) –x+1/2, -y+1/2, -z+1; (ii) x, -y, z+1/2; (iii) x, -y+1, z-1/2.

Interaction between complex 1 and DNA: The CV of complex **1** and DNA was shown in Fig. 2. An oxidation peak was observed at the glassy carbon electrode. The anodic peak potential E_{pa} was 0.390 V and its formal potential (E^0) is 0.496 V.

To study the interaction between complex **1** and DNA, the DPV of complex **1** before and after adding DNA was also recorded, as shown in Fig. 3. Curve a is the DPV of complex **1** in the absence of DNA, while curve b is the DPV of complex **1** in the presence of DNA. No new oxidation peak appeared after adding DNA, but the oxidation current peak was obviously decreased after adding DNA. So the initial conclusion can be obtained that complex **1** can interact with DNA.

Interaction between complex 2 and DNA: Fig. 4 shows the CV of complex **2** with or without DNA. A couple of redox peaks was observed at the glassy carbon electrode. The cathodic peak potential E_{pc} and anodic peak potential E_{pa} were -0.008 and 0.028 V, respectively. The separation of the cathodic and the anodic peak potentials (ΔE_p) was 20 mV quasi-reversible redox process.

The DPV of complex **2** before and after adding DNA was recorded to test whether complex **2** interacted with DNA or not. DPV of complex **2** in the presence or absence of DNA at the glassy carbon electrode (GCE) is shown in Fig. 5. Curve a is the DPV of complex **2** in the absence of DNA, while curve b is the DPV of complex **2** in the presence of DNA. No new oxidation peak appeared after adding DNA, but the oxidation current peak was obviously decreased after adding DNA. The initial conclusion can be also drawn that complex **2** can interact with DNA.

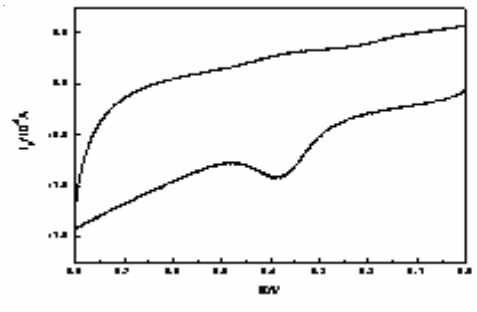

Fig. 2 Cyclic voltammogram (CV) of complex **1** in 0.2 mol/L phosphate buffer solution at pH 4.5. Scan rate: 0.1 V/s, quiet time: 2 s

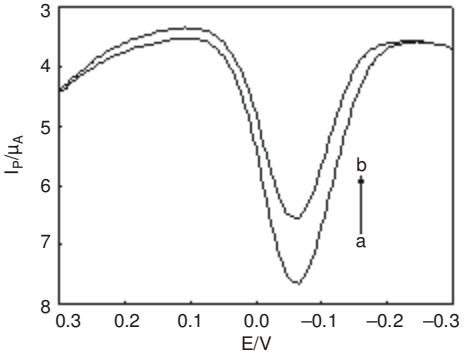

Fig. 3. Differential pulse voltammograms (DPV) of complex 1 in the absence or presence of DNA with c_1: 1.0×10^{-5} mol/L, c_{DNA}: (a) 0 (b) 1.68×10^{-5} mol/L. Scan rate: 0.1 V/s, quiet time: 2 s

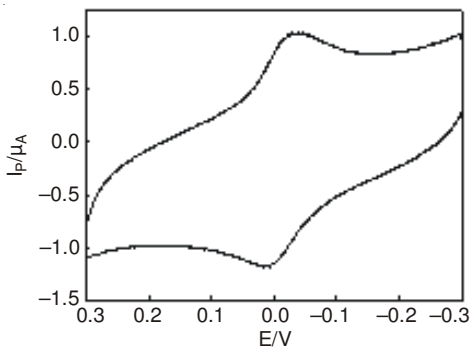

Fig. 4. Cyclic voltammogram (CV) of complex **2** in 0.2 mol/L HOAc-NaOAc buffer solution at pH 5.0. Scan rate: 0.1 V/s, quiet time: 2 s

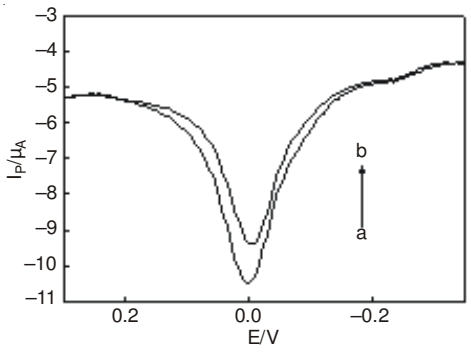

Fig. 5. Differential pulse voltammograms (DPV) of complex **2** in the absence or presence of DNA with c_1: 1.0×10^{-4} mol/L, c_{DNA}: (a) 0 (b) 1.68×10^{-5} mol/L. Scan rate: 0.1 V/s, quiet time: 2 s

Fig. 6 shows the CVs of GCE in 0.2 mol/L HOAc-NaOAc buffer solution (pH 5.0) containing 0.001 mol/L complex **2** at different scan rates. A pair of roughly symmetric anodic and cathodic peaks appeared with almost equal peak currents in the scan rate range from 30 to 300 mV/s. It can be seen that the potential and peak current are dependent on the scan rate. The peak-to-peak separation also increased with the scan rate. In the scan rate range of 30 to 300 mV/s, the reduction peak currents rise linearly with increased scan rates, with a correlation coefficient of 0.997 (upper left inset), suggesting that the reaction is a surface-controlled process.

Fig. 7 shows the DPVs for $Fe_2(C_{14}H_{12}N_2)_2(C_4H_2O_4^{2-})(NO_3^-)_4{\cdot}2H_2O$ in solution at the bare GCE, ssDNA/GCE and dsDNA/GCE, respectively. The $Fe_2(C_{14}H_{12}N_2)_2$-$(C_4H_2O_4^{2-})(NO_3^-)_4{\cdot}2H_2O$ signal obtained with the bare GCE (curve a in Fig. 7) was larger than those obtained with the ssDNA/GCE (curve b in Fig. 7) and dsDNA/

GCE (curve c in Fig. 7), while the potential were almost unchanged. The decrease in the voltammetric signal obtained from the dsDNA-modified GCE was attributed to the accumulation of the indicator at the electrode surface as a result of the interaction of the planar ring into the dsDNA helix[31]. The electrochemically active metal centers of $Fe_2(C_{14}H_{12}N_2)_2(C_4H_2O_4^{2-})(NO_3^-)_4{\cdot}2H_2O$ were enveloped by the bulkyl DNA molecule on the GCE surface and the singal of $Fe_2(C_{14}H_{12}N_2)_2(C_4H_2O_4^{2-})(NO_3^-)_4{\cdot}2H_2O$ was thus reduced. In addition, the shifts in the DPV peal potentials for the electroactive indicators can indicate the mode of the interaction of DNA with the indicators[32].

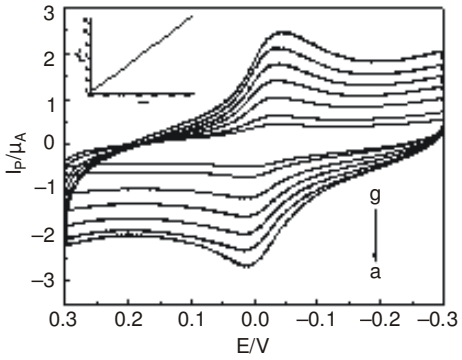

Fig. 6. Cyclic voltammograms (CV) of GCE in 0.2 mol/L HOAc-NaOAc buffer solution (pH 5.0) containing 0.001 mol/L complex **2** at (a) 30 mV/s; (b) 50 mV/s; (c) 100 mV/s; (d) 150 mV/s; (e) 200 mV/s; (f) 250 mV/s; (g) 300 mV/s

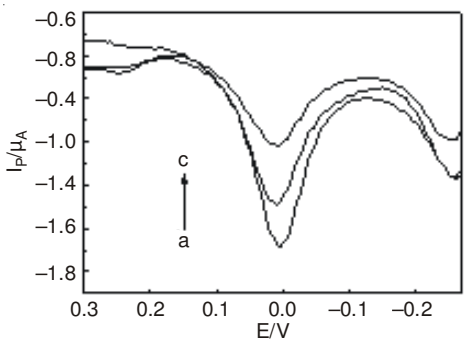

Fig. 7. Differential pulse voltammograms (DPV) of bare GCE (a), ssDNA/GCE (b), dsDNA /GCE (c) in 0.2 mol/L HOAc-NaOAc buffer solution (pH 5.0) containing 0.001 mol/L complex **2**

Thermal analysis of complex 2: The thermal stability of complexes is very important for their potential use in biology. Thermogravimetric analysis is a significant dynamic way of detecting degradation behaviour, the weight loss of a complex sample is measured continuously, whereas the temperature is changed at a constant way. In order to evaluate the thermal stability of complex **2**, the thermal analysis of complex **2** was tested as shown in Fig. 8. The thermal analysis was performed under a nitrogen steam in the temperature of 12-600 ºC with a heating rate of 10 ºC/min.

As shown in Fig. 8, the degradation rate can reach maximum at the temperature of 178.5 ºC. Thermal decomposition started with endothermic step in the range of 60-98 ºC and the weight loss of the complex **2** was nearly equal to *ca.* 3.45 % in this range. This degradation can be ascribed to the evaporation of coordinated water in the complex **2**. In the second step (98-150 ºC), there was a slight weight loss of 9.48 %, which may be caused by degradation and volatilization of fumarate. It can be seen clearly that there was an evident degradation process for complex **2** occurred at the range 150-205 ºC. The prominent weight losses were caused by the release process of 2,9-dimethyl-1,10-phenanthroline. The last weight loss (205-500 ºC) indicated

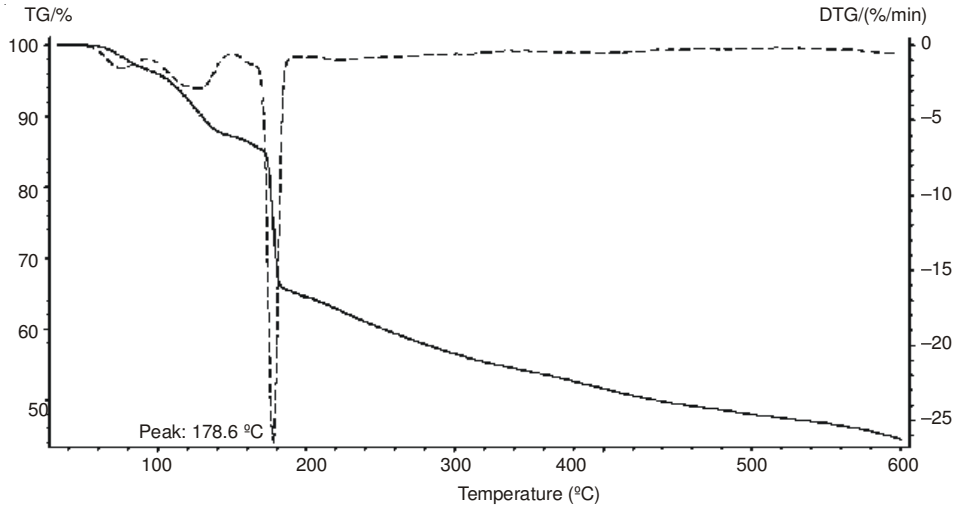

Fig. 8. TG-DTG thermal analysis curves of complex **2**

$Fe(NO_3)_3$ dissociation process. Based on these results described above, it can reasonably draw the conclusion that complex **2** is good thermal stability for the application.

Conclusion

Two novel transition metal complexes containing phen and fumarate had been synthesized and characterized. The crystal structure of complex **1** was determined by X-ray crystallography. And the structure of complex **2** has been analyzed by EA and ^{1}H NMR. TGA result indicates that complex **2** has good thermal stability. From the result of the electrochemical study, initial conclusion can be drawn that complex **1** and **2** can interact with DNA. Thus, the transition metal complexes might have the potential use as indicators of biosensors.

ACKNOWLEDGEMENTS

The authors would like to acknowledge the financial support of this work by the Natural Science Foundation of Shandong Province, China (Y2006B07), the Key Technologies R&D Program of Shandong of Shandong Province, China (2006 GG2203024) and the Program for New Century Excellent Talents in University (No. NCET-04-0649).

REFERENCES

1. R. Zicssel, A. Harriman, J. Suffort, M.T. Youinou, A. Dccian and J. Fischer, *Angew. Chem., Int. Ed. Engl.*, **36**, 2509 (1997).
2. C.O. Dietrich-Buchecker and J.P. Sauvage, *Angew. Chem., Int. Ed. Engl.*, **28**, 189 (1989).
3. F. Sallas, A. Marsura, V. Petot, I. Pinter, J. Kovacs and L. Jicisinszky, *Helv. Chim. Acta*, **81**, 632 (1998).
4. A. Moghimi, R. Alizadeh and A. Shokrollahi, *Inorg. Chem.*, **42**, 1616 (2003).
5. Z.M. Wang, H.K. Lin and S.R. Zhu, *Anti-Cancer Drug Des.*, **15**, 405 (2000).
6. H. Skurai, H. Tamura and K. Okatani, *Biochem. Biophys. Res. Commun.*, **206**, 133 (1995).

7. Z.M. Wang, H.K. Lin and Z.F. Zhou, *Bioorg. Med. Chem.*, **9**, 2849 (2001).
8. P.J. Dardlier, R.E. Holmlin and J.K. Barton, *Science*, **275**, 1465 (1997).
9. D.B. Hall, R.E. Holmlin and J.K. Barton, *Nature*, **382**, 731 (1996).
10. M.V. Keek and S. Lippard, *J. Am. Chem. Soc.*, **114**, 3386 (1992).
11. A.E. Friedman, J.C. Chamborn, J.P. Sauvage, N.J. Turrro and J.K. Barton, *J. Am. Chem. Soc.*, **114**, 5919 (1992).
12. R.M. Hartshorm and J.K. Barton, *J. Am. Chem. Soc.*, **112**, 4960 (1990).
13. A.S. Sitlani, E.C. Long, A.M. Pyle and J.K. Barton, *J. Am. Chem. Soc.*, **114**, 2230 (1992).
14. D.S. Sigman, A. Mazumder and D.M. Perrin, *Chem. Rev.*, **93**, 2295 (1993).
15. G. Pratvicl, J. Bernadou and B. Mcunicr, *Adv. Inorg. Chem.*, **45**, 251 (1998).
16. L.N. Ji, X.H. Zou and J.G. Liu, *Coord. Chem. Rev.*, **216**, 513 (2001).
17. J.A. Cowan, *Curr. Opin. Chem. Biol.*, **5**, 634 (2001).
18. C.V. Kumar, J.K. Barton and N.J. Turro, *J. Am. Chem. Soc.*, **107**, 5518 (1985).
19. H. Xu, K.C. Zheng, H. Deng, L.J. Lin, Q.L. Zhang and L.N. Ji, *J. Chem. Soc., Dalton. Trans.*, 2260 (2003).
20. S. Mahadevan and M. Palaniandavar, *Inorg. Chim. Acta*, **254**, 291 (1997).
21. H. Xu, K.C. Zheng, H. Deng, L.J. Lin, Q.L. Zhang and L.N. Ji, *New J. Chem.*, **27**, 1255 (2003).
22. A. Mozaffar, S. Elham, R. Bijian and H. Leila, *New J. Chem.*, **28**, 1227 (2004).
23. J.B. Chaires, *Biopolymers*, **44**, 201 (1998).
24. A. Pasini and F. Zunino, *Angew. Chem. Int. Ed. Engl.*, **26**, 615 (1987).
25. J.K. Barton, *Science*, **233**, 727 (1986).
26. J. Wang, X. Cai, G. Rivas, H. Shiraishi and P.A.M. Farias, *Anal. Chem.*, **68**, 2629 (1996).
27. J. Pfau, D.N. Arvidson, P. Yuderian, L.L. Pearson and D.S. Sigman, *Biochemistry*, **68**, 2629 (1994).
28. Y. Ni, D. Lin and S. Kokot, *Anal. Biochem.*, **352**, 231 (2006).
29. S. Dhar, M. Nrthaji and A.R. Chakravaty, *Inorg. Chim. Acta*, **358**, 2437 (2005).
30. S. Dhar, D. Senapati, P.K. Das, P. Chattopadhyay, M. Nethaji and A.R. Chakravaty, *J. Am. Chem. Soc.*, **125**, 12118 (2003).
31. X.M. Li, H.Q. Ju, L.P. Du and S.S. Zhang, *J. Inorg. Biochem.*, **101**, 1165 (2007).
32. M.T. Carter, M. Rodriguez and A.J. Bard, *J. Am. Chem. Soc.*, **111**, 8901 (1989).

(*Received*: 24 May 2008; *Accepted*: 1 October 2009) AJC-7922